ETH
Eidgenössische Technische Hochschule Zürich
Swiss Federal Institute of Technology Zurich

Seminar for Applied Mathematics SAM

Trefftz Co-chain Calculus

D. Casati and L. Codecasa and R. Hiptmair and F. Moro

Research Report No. 2019-19

April 2019
Latest revision: August 2019

Seminar für Angewandte Mathematik
Eidgenössische Technische Hochschule
CH-8092 Zürich
Switzerland

Funding SNF: 2000021_165674/1

Trefftz Co-Chain Calculus

Daniele Casati[a,*], Lorenzo Codecasa[b], Ralf Hiptmair[a], Federico Moro[c]

[a] *Seminar for Applied Mathematics, ETH Zurich, Switzerland*
[b] *Dipartimento di Elettronica, Informazione e Bioingegneria, Politecnico di Milano, Italy*
[c] *Dipartimento di Ingegneria Industriale, Università degli Studi di Padova, Italy*

Abstract

We propose a comprehensive approach to obtain systems of equations that discretize linear stationary or time-harmonic elliptic problems in unbounded domains. This is achieved by coupling any numerical method that fits co-chain calculus with a Trefftz method.

The framework of co-chain calculus accommodates both finite element exterior calculus and discrete exterior calculus. It encompasses methods based on volume meshes: its application is therefore confined to bounded domains.

Conversely, Trefftz methods are based on functions that solve the homogeneous equations exactly in the unbounded complement of the meshed domain, while satisfying suitable conditions at infinity. An example of a Trefftz method is the Multiple Multipole Program (MMP), which makes use of multipoles, i.e. solutions spawned by point sources with central singularities that are placed outside the domain of approximation. In our approach the degrees of freedom describing these sources can be eliminated by computing the Schur complement of the system for the coupling, therefore leading to a boundary term for co-chain calculus that takes into account the exterior problem.

As a concrete example, we specialize this general framework for the cell method, a particular variant of discrete exterior calculus, coupled with MMP to solve frequency-domain eddy-current problems. A numerical experiment shows

*Corresponding author
Email addresses: daniele.casati@sam.math.ethz.ch (Daniele Casati), lorenzo.codecasa@polimi.it (Lorenzo Codecasa), ralf.hiptmair@sam.math.ethz.ch (Ralf Hiptmair), federico.moro@unipd.it (Federico Moro)

the effectiveness of this approach.

Keywords: co-chain calculus, finite element exterior calculus, discrete exterior calculus, cell method, Trefftz method, multiple multipole program
2010 MSC: 35Q61, 65N30, 65N80, 65Z05

1. Introduction

The framework of *co-chain calculus* [1, 2] allows for a unified treatment of a wide class of finite element and finite volume schemes, building on the foundation established by other works like [3]. This framework is the generalization of both *Finite Element Exterior Calculus* (FEEC) [4] and *Discrete Exterior Calculus* (DEC) [5, 6]. The degrees of freedom of the former are coefficients of an expansion in terms of piecewise polynomials built on a mesh: what one obtains is a function approximating the unknown in the chosen functional space, in the way of *Finite Element Methods* (FEM). Conversely, DEC operates on values of the unknown on entities of (primal and dual) meshes, something more akin to finite difference or finite volume methods.

The starting point of co-chain calculus is a linear stationary or time-harmonic elliptic boundary value problem, expressed in terms of differential forms and *Hodge operators* (see Section 2). In particular, we distinguish between *equilibrium equations*, stated by means of the exterior derivative, and *constitutive equations*, involving Hodge operators. In the discrete setting, based on meshes, Hodge operators are approximated by matrices, whose construction is done differently in FEEC and DEC, as discussed in [1, Section 4]. However, the discrete matrix forms of co-chain calculus need to respect only a few algebraic requirements, independent of the details of the approximation. These are only addressed when the framework of co-chain calculus is specialized into a numerical method.

[0] *Abbreviations.* FEEC: Finite Element Exterior Calculus. DEC: Discrete Exterior Calculus. FEM: Finite Element Method. BEM: Boundary Element Method. MMP: Multiple Multipole Program. DtN: Dirichlet-to-Neumann.

Moreover, in order to include both FEEC and DEC, the discrete formalism of co-chain calculus is based on both a primary and a secondary mesh on a bounded domain. Given a numerical method, if its degrees of freedom are defined on either the primary or secondary mesh, we disregard the other mesh and fit the method into FEEC. Conversely, some degrees of freedom may be represented on the primary mesh and others on the secondary mesh. In this case, a bijective relationship between the two types of unknowns is needed, which can be achieved by using a secondary mesh *dual* to the primary mesh. This leads to numerical schemes fitting the framework of DEC, which are called *generalized finite volume methods* in [2], *generalized finite differences* in [3], and *cell method* in [7].

1.1. Cell Method

The cell method, established by [7], relies on a pair of meshes for the spatial discretization of boundary value problems: one mesh being the dual of the other. A Delaunay–Voronoi subdivision for the dual mesh is proposed in [8], whereas barycentric dual meshes are used in [9, 10, 11, 12].

Degrees of freedom of the cell method are integrals on entities of the primal and dual meshes. In the context of electromagnetics, where the cell method has long been used, examples are fluxes of the magnetic flux density on primal faces or line integrals of the magnetic field on dual edges [8]. This allows rewriting differential operators applied to fields in integral form as incidence matrices between integrals on entities of the meshes, by using Stokes' theorem [13, p. 31]. In this way, equilibrium equations can be enforced exactly.

Basis functions are required to interpolate fields locally in terms of these integral degrees of freedom and then approximate the material laws (constitutive equations). With the choice of Whitney basis functions, the matrices of FEEC can be recovered [7, 8]. Piecewise-constant basis functions [14] are used in [11, 12] to interpolate on generic mesh entities (any polyhedron is allowed [15]), thus leading to more applications than FEM. Moreover, [9] overcomes some limitations of the original cell method, namely how to take into account boundary

conditions and energetic quantities, by means of augmented dual meshes.

Starting from [9], the cell method has been coupled with the Boundary Element Method (BEM) for magnetostatic [11] and eddy-current problems [12]. Both works end up with symmetric linear systems analogous to the one explored in this work (Section 3.2), which can be handled by iterative solvers. However, those systems also contain a large, dense diagonal block due to BEM, whose inverse cannot be computed explicitly [16] if one wants to reduce the size of the final coupling system by a Schur complement approach. On the other hand, when coupled with techniques based on volume meshes, *Trefftz methods* lead to small and, for some configurations, even diagonal blocks.

1.2. Trefftz Methods

Trefftz methods seek to approximate the solution of boundary value problems in (unbounded) domains by means of global basis functions that solve the homogeneous equations of the problem exactly and satisfy suitable conditions at infinity [17].

Specifically, the *Multiple Multipole Program* (MMP) employs *multipoles*, which are solutions spawned by point sources with central singularities that are placed outside the domain of approximation [18]. This is why MMP belongs to the class of methods of auxiliary sources. In a spherical coordinate system with shifted origin, a multipole can be factored into a radial part, which includes a singularity at the new origin (the center of the multipole) and the desired behavior at infinity, and a spherical part, formulated in terms of (vector) spherical harmonics [19].

The discrete equations of a Trefftz method arise from imposing boundary conditions on hypersurfaces, and the obtained linear combination of Trefftz basis functions gives an approximate solution in the whole domain where the equations hold. The discrete equations are obtained by collocation and generally yield an ill-conditioned overdetermined system [18]. However, Trefftz functions can be made orthogonal by a change of basis [20] or by choosing them orthogonal in the first place (see Section 4).

Trefftz methods have already been coupled with FEM in [21, 22] for Poisson's equation and [23] for Maxwell's equations. The coupling proposed in this work between co-chain calculus and Trefftz functions can be seen as a generalization of the *Dirichlet-to-Neumann-based* (DtN-based) *coupling* presented in [21, Section 3.2].

1.3. Outline of This Work

Section 2 presents co-chain calculus for a linear stationary or time-harmonic elliptic boundary value problem, while Section 2.1 illustrates its coupling with a Trefftz method. Section 2.2 replaces the equations for the exterior problem with a simpler, but equivalent expression, given some conditions on the topology of the Trefftz domain that can always be satisfied.

Correspondingly, Section 3 specializes Section 2 for the cell method applied to frequency-domain eddy-current problems, while Section 3.1 illustrates its coupling with a Trefftz method. Section 3.2 solves the exterior problem with a magnetic scalar potential, special case of the approach of Section 2.2, and gives explicit formulas for the related Trefftz functions (which are multipoles).

Finally, numerical tests based on the formulation of Section 3.2 are reported in Section 4.

2. Co-Chain Calculus for Elliptic Boundary Value Problems

We write $\Lambda^l(\mathbb{R}^n)$ for the space of differential forms of order l, $0 \leq l \leq n$, in $\mathbb{R}^n$, $n \in \mathbb{N}^*$ [4, p. 13, Section 2.2].

The statement of an elliptic boundary value problem is composed of two sets of equations. One is the set of equilibrium equations

$$\begin{cases} \mathrm{d}u = (-1)^l \boldsymbol{\sigma}, \\ \mathrm{d}\mathbf{j} = \psi, \end{cases} \tag{1a}$$

connecting the differential forms $u \in \Lambda^{l-1}(\mathbb{R}^n)$, $\boldsymbol{\sigma} \in \Lambda^{l}(\mathbb{R}^n)$, $\mathbf{j} \in \Lambda^{m}(\mathbb{R}^n)$, $\psi \in \Lambda^{m+1}(\mathbb{R}^n)$ for $l \in \{1, \dots, n\}$ and $m := n - l$. The other set is formed by the constitutive equations

$$\begin{cases} \mathbf{j} = \star_\alpha \boldsymbol{\sigma}, \\ \psi = \star_\gamma u \,. \end{cases} \tag{1b}$$

The symbols $\star_\alpha$ and $\star_\gamma$ indicate *Hodge operators*, which supply linear mappings of l-forms into m-forms [4, p. 12]. These are induced by the Riemannian metrics α and γ: if $\mathbb{R}^n$ is equipped with Cartesian coordinates, these metrics can be represented by Hermitian positive-definite[1] matrix fields.

The problem is completed by the condition at infinity [24, p. 259, Theorem 8.9]

$$\|u(\mathbf{x})\| = \begin{cases} C \log\|\mathbf{x}\| + \mathcal{O}(\|\mathbf{x}\|^{-1}),\ C \in \mathbb{C} & \text{if } n = 2 \\ \mathcal{O}(\|\mathbf{x}\|^{2-n}) & \text{if } n \geq 3 \end{cases} \quad \text{for } \|\mathbf{x}\| \to \infty \text{ uniformly.} \tag{2}$$

For the sake of simplicity, we consider a bounded domain $\Omega_\star$ such that, in the complement $\mathbb{R}^n \setminus \Omega_\star$, we have constant $\alpha, \gamma \in \mathbb{C}$. Let us also introduce $\Omega \supset \Omega_\star$, in whose complement $\mathbb{R}^n \setminus \Omega$ we are given a known nonzero excitation $(l-1)$-form w such that $u|_{\mathbb{R}^n \setminus \Omega} = v + w$, with $v, w \in \Lambda^{l-1}(\mathbb{R}^n \setminus \Omega)$ and v solving the homogeneous problem. The field w will enter the right-hand side of the system.

Furthermore, we assume that $\gamma = 0$ in $\mathbb{R}^n \setminus \Omega$, which implies $\psi|_{\mathbb{R}^n \setminus \Omega} = 0$ and $\mathrm{d}\mathbf{j}|_{\mathbb{R}^n \setminus \Omega} = 0$ from (1a) and (1b).

Next, we eliminate all other variables except for u in Ω:

$$\mathrm{d}\left(\star_\alpha \mathrm{d}u\right) = (-1)^l \,\mathrm{d}\left(\star_\alpha \boldsymbol{\sigma}\right) = (-1)^l \,\mathrm{d}\mathbf{j} = (-1)^l \,\psi = (-1)^l \star_\gamma u \,, \tag{3}$$

which can be rewritten as

$$(-1)^{l-1} \,\mathrm{d}\left(\star_\alpha \mathrm{d}u\right) + \star_\gamma u = 0 \,. \tag{4}$$

[1] γ can also be expressed by a Hermitian positive-definite matrix scaled by a complex scalar, which is the case of Section 3.

Multiplication with $\eta \in \Lambda^{l-1}(\Omega)$ and integration on Ω yields

$$\int_\Omega \left[(-1)^{l-1}\,\mathrm{d}\,(\star_\alpha \mathrm{d}u) + \star_\gamma u\right] \wedge \eta = 0 \quad \forall \eta \in \Lambda^{l-1}(\Omega). \tag{5}$$

Taking the $\wedge$-product with η and integrating by parts [2, p. 254, (6)], we then obtain the weak formulation

$$\int_\Omega (\star_\alpha \mathrm{d}u \wedge \mathrm{d}\eta + \star_\gamma u \wedge \eta) + (-1)^{l-1} \int_\Gamma \mathbf{t}\,(\star_\alpha \mathrm{d}u) \wedge \mathbf{t}\,\eta = 0 \quad \forall \eta \in \Lambda^{l-1}(\Omega), \tag{6}$$

where $\mathbf{t} : \Lambda^l(\Omega) \to \Lambda^l(\Gamma)$ is the (tangential, Dirichlet) trace of l-forms for any $l \in \{1, \ldots, n\}$ on $\Gamma := \partial\Omega$.

2.1. Coupling with a Trefftz Method through an $(l-1)$-Form

We discretize Hodge operators inside Ω (approximation of constitutive equations), while we use Trefftz functions in the complement $\Omega_\mathrm{T} := \mathbb{R}^3 \setminus \Omega$, i.e. functions that belong to the *Trefftz space*

$$\begin{aligned}\mathcal{T}(\Omega_\mathrm{T}) := \Big\{ & v \in \Lambda^{l-1}(\Omega_\mathrm{T}) \colon \ \mathrm{d}\,(\star_\alpha \mathrm{d}v) = 0\,, \ \ \alpha \in \mathbb{C}, \\ & v \text{ satisfies the condition at infinity (2)} \Big\}.\end{aligned} \tag{7}$$

Transmission conditions are required between Ω and Ω_T [25, p. 107, Lemma 5.3]:

$$\begin{cases} \mathbf{t}\left(\star_\alpha \mathrm{d}u|_\Omega\right) = \mathbf{t}\left(\star_\alpha \mathrm{d}u|_{\Omega_\mathrm{T}}\right) & \text{on } \Gamma. \quad (8a) \\ \mathbf{t}\,u|_\Omega = \mathbf{t}\,u|_{\Omega_\mathrm{T}} & (8b) \end{cases}$$

From now on, with a small abuse of notation, we refer to $u|_\Omega$ as u. We also write $u|_{\Omega_\mathrm{T}} := v + w$, where $v \in \mathcal{T}(\Omega_\mathrm{T})$ and w is the known excitation $(l-1)$-form.

We then plug (8a) into (6) and impose (8b) weakly with test functions in $\mathcal{T}(\Omega_\mathrm{T})$ to obtain the system for the coupling:

$$\boxed{\begin{aligned} &\text{Seek } \ u \in \Lambda^{l-1}(\Omega), \ \ v \in \mathcal{T}(\Omega_\mathrm{T})\colon \\ &\int_\Omega (\star_\alpha \mathrm{d}u \wedge \mathrm{d}\eta + \star_\gamma u \wedge \eta) + (-1)^{l-1} \int_\Gamma \mathbf{t}\,(\star_\alpha \mathrm{d}v) \wedge \mathbf{t}\,\eta = (-1)^{l} \int_\Gamma \mathbf{t}\,(\star_\alpha \mathrm{d}w) \wedge \mathbf{t}\,\eta \\ &(-1)^{l-1} \int_\Gamma \mathbf{t}\,(\star_\alpha \mathrm{d}\zeta) \wedge \mathbf{t}\,u - (-1)^{l-1} \int_\Gamma \mathbf{t}\,(\star_\alpha \mathrm{d}\zeta) \wedge \mathbf{t}\,v = (-1)^{l-1} \int_\Gamma \mathbf{t}\,(\star_\alpha \mathrm{d}\zeta) \wedge \mathbf{t}\,w \\ &\qquad \forall \eta \in \Lambda^{l-1}(\Omega),\ \forall \zeta \in \mathcal{T}(\Omega_\mathrm{T}). \end{aligned}} \tag{9}$$

We choose primary and secondary discretization meshes which can be unrelated [2, p. 250, Definition 2.2]. From now on, quantities related to the secondary mesh are tagged by a tilde. Then, with the discrete counterpart of the integration by parts formula used in (6), we can rewrite (9) in abstract algebraic form

$$\boxed{\begin{array}{lll} \left[\left(\mathbf{D}^{l-1}\right)^{\mathsf{H}} \mathbf{M}_{\alpha}^{l} \mathbf{D}^{l-1} + \mathbf{M}_{\gamma}^{l-1}\right] \vec{\mathbf{u}} + (-1)^{l-1} \left(\mathbf{T}_{\Gamma}^{l-1}\right)^{\mathsf{H}} \widetilde{\mathbf{K}}_{m,\Gamma}^{l-1} \mathbf{P}_{\Gamma} \vec{\mathbf{v}} = (-1)^{l} \left(\mathbf{T}_{\Gamma}^{l-1}\right)^{\mathsf{H}} \widetilde{\mathbf{K}}_{m,\Gamma}^{l-1} \vec{\boldsymbol{\omega}} \\ (-1)^{l-1} \mathbf{P}_{\Gamma}^{\mathsf{H}} \left(\widetilde{\mathbf{K}}_{m,\Gamma}^{l-1}\right)^{\mathsf{H}} \mathbf{T}_{\Gamma}^{l-1} \vec{\mathbf{u}} - \mathbf{M}_{\mathrm{T}} \vec{\mathbf{v}} = (-1)^{l-1} \mathbf{P}_{\Gamma}^{\mathsf{H}} \left(\widetilde{\mathbf{K}}_{m,\Gamma}^{l-1}\right)^{\mathsf{H}} \vec{\mathbf{w}} \end{array}} \tag{10}$$

using the following terms:

- The *exterior-derivative* matrix $\mathbf{D}^{l-1} \in \{-1, 0, 1\}^{N_l, N_{l-1}}$, with N_l number of l-dimensional entities of the primary mesh, is the incidence matrix between oriented l- and $(l-1)$-dimensional entities.
- *Mass* matrices $\mathbf{M}_{\alpha}^{l} \in \mathbb{C}^{N_l, N_l}$ and $\mathbf{M}_{\gamma}^{l-1} \in \mathbb{C}^{N_{l-1}, N_{l-1}}$ need to be square, Hermitian, and positive-definite[2] [2, p. 254]. They can be viewed as discrete Hodge operators.
- We use a vector notation for the coefficient vector $\vec{\mathbf{u}} \in \mathbb{C}^{N_{l-1}}$, whose entries are related to integrals of $u \in \Lambda^{l-1}(\Omega)$ over the $(l-1)$-dimensional entities of the primary mesh. These integrals are regarded as *degrees of freedom*.
- The *trace* matrix $\mathbf{T}_{\Gamma}^{l-1} \in \{0, 1\}^{N_{l-1}^{\mathrm{bnd}}, N_{l-1}}$, with N_{l-1}^{bnd} number of $(l-1)$-dimensional primary mesh entities $\subset \Gamma$, selects the degrees of freedom on Γ.
- The *pairing* matrix $\widetilde{\mathbf{K}}_{m,\Gamma}^{l-1} \in \mathbb{C}^{N_{l-1}^{\mathrm{bnd}}, \widetilde{N}_{m}^{\mathrm{bnd}}}$ is a discrete representative of the $\wedge$-product $\int_{\Gamma} f \wedge g$, $f \in \Lambda^{l-1}(\Omega)$, $g \in \Lambda^{m}(\Omega)$. Pairing matrices need to fulfill the algebraic relationship [2, p. 254]

$$\widetilde{\mathbf{K}}_{m}^{l} = (-1)^{lm} \left(\mathbf{K}_{l}^{m}\right)^{\mathsf{H}} \iff \mathbf{K}_{l}^{m} = (-1)^{lm} \left(\widetilde{\mathbf{K}}_{m}^{l}\right)^{\mathsf{H}} \tag{11}$$

[2] $\mathbf{M}_{\gamma}^{l-1}$ can also be a square Hermitian positive-definite matrix scaled by a complex scalar, which is the case of Section 3.1.

for any $l \in \{1, \ldots, n\}$, $m := n - l$.

- We call $\mathbf{P}_\Gamma \in \mathbb{C}^{\widetilde{N}_m^{\mathrm{bnd}}, N_\mathrm{T}}$ *Dirichlet-to-Neumann* (DtN) matrix, with N_T dimension of the discrete Trefftz space $\mathcal{T}_n(\Omega_\mathrm{T}) \in \mathcal{T}(\Omega_\mathrm{T})$. Comparing (9) and (10), it stands clear that the role of $\mathbf{P}_\Gamma$ is to connect the discrete representations of v and $\star_\alpha \mathrm{d} v$ (the latter expressed only by degrees of freedom on Γ).

- $\vec{\mathbf{v}} \in \mathbb{C}^{N_\mathrm{T}}$ is the vector of expansion coefficients of $v \in \mathcal{T}_n(\Omega_\mathrm{T})$ with respect to a basis of the discrete Trefftz space.

- $\vec{\mathbf{w}} \in \mathbb{C}^{N_{l-1}^{\mathrm{bnd}}}$ and $\vec{\boldsymbol{\omega}} \in \mathbb{C}^{\widetilde{N}_m^{\mathrm{bnd}}}$ are known vectors determined by integrals of the excitation $(l-1)$-form w on $(l-1)$-entities of the primary mesh and by $\star_\alpha \mathrm{d} w$ on m-entities of the secondary mesh, respectively.

- $\mathbf{M}_\mathrm{T} \in \mathbb{C}^{N_\mathrm{T}, N_\mathrm{T}}$ is the *energy* matrix in Ω_T, another discrete Hodge operator. This interpretation is clarified below.

We deduce an expression with the energy matrix in Ω_T based on the discrete form of (6), which is also given in [2, p. 255, *Primary elimination*, (12)]. There, the left-hand side of the resulting linear system is

$$\left[\left(\mathbf{D}^{l-1}\right)^\mathsf{H} \mathbf{M}_\alpha^l \mathbf{D}^{l-1} + \mathbf{M}_\gamma^{l-1} + \left(\mathbf{T}_\Gamma^{l-1}\right)^\mathsf{H} \mathbf{M}_{\beta,\Gamma}^{l-1} \mathbf{T}_\Gamma^{l-1} \right] \vec{\mathbf{u}}\,, \tag{12}$$

where $\mathbf{M}_{\beta,\Gamma}^{l-1}$ is an abstract *boundary-energy* term related to the DtN operator.

To arrive at an expression involving $\mathbf{M}_\mathrm{T} \in \mathbb{C}^{N_\mathrm{T}, N_\mathrm{T}}$, we note that the total number of degrees of freedom of the Trefftz discretization, N_T, is generally low because, under certain conditions, Trefftz methods enjoy exponential convergence [21, 26]. Thus, $\mathbf{M}_\mathrm{T}$ can easily be inverted by Gaussian elimination, and we can write the Schur complement of (10):

$$\boxed{\begin{aligned} &\left[\left(\mathbf{D}^{l-1}\right)^\mathsf{H} \mathbf{M}_\alpha^l \mathbf{D}^{l-1} + \mathbf{M}_\gamma^{l-1} + \left(\mathbf{T}_\Gamma^{l-1}\right)^\mathsf{H} \widetilde{\mathbf{K}}_{m,\Gamma}^{l-1} \mathbf{P}_\Gamma \mathbf{M}_\mathrm{T}^{-1} \mathbf{P}_\Gamma^\mathsf{H} \left(\widetilde{\mathbf{K}}_{m,\Gamma}^{l-1}\right)^\mathsf{H} \mathbf{T}_\Gamma^{l-1} \right] \vec{\mathbf{u}} = \\ &\qquad (-1)^l \left(\mathbf{T}_\Gamma^{l-1}\right)^\mathsf{H} \widetilde{\mathbf{K}}_{m,\Gamma}^{l-1} \vec{\boldsymbol{\omega}} + \left(\mathbf{T}_\Gamma^{l-1}\right)^\mathsf{H} \widetilde{\mathbf{K}}_{m,\Gamma}^{l-1} \mathbf{P}_\Gamma \mathbf{M}_\mathrm{T}^{-1} \mathbf{P}_\Gamma^\mathsf{H} \left(\widetilde{\mathbf{K}}_{m,\Gamma}^{l-1}\right)^\mathsf{H} \vec{\mathbf{w}}. \end{aligned}} \tag{13}$$

We can now compare the left-hand side of (13) with the generic discrete system (12), write

$$\mathbf{M}^{l-1}_{\beta,\Gamma} \equiv \widetilde{\mathbf{K}}^{l-1}_{m,\Gamma} \mathbf{P}_\Gamma \mathbf{M}^{-1}_{\mathrm{T}} \mathbf{P}^{\mathsf{H}}_\Gamma \left(\widetilde{\mathbf{K}}^{l-1}_{m,\Gamma} \right)^{\mathsf{H}}, \tag{14}$$

and associate the boundary-energy term of (13) with the energy in Ω_{T}: both matrices are discrete Hodge operators, like mass matrices $\mathbf{M}^l_\alpha, \mathbf{M}^{l-1}_\gamma$. More details on this association are given in the next paragraph.

Remark. The system (9) can also be derived by finding a stationary point of the functional

$$\begin{aligned} \mathcal{L}(u,v) := \frac{1}{2} \int_\Omega \left(\star_\alpha \mathrm{d}u \wedge \mathrm{d}u + \star_\gamma u \wedge u \right) + \frac{1}{2} \int_{\Omega_{\mathrm{T}}} \star_\alpha \mathrm{d}\left(v+w\right) \wedge \mathrm{d}\left(v+w\right) + \\ (-1)^{l-1} \int_\Gamma \mathbf{t}\left[\star_\alpha \mathrm{d}\left(v+w\right) \right] \wedge \mathbf{t}\, u\,, \end{aligned} \tag{15}$$

with $u \in \Lambda^{l-1}(\Omega)$ and $v, w \in \mathcal{T}(\Omega_{\mathrm{T}})$, where w is the known excitation $(l-1)$-form.

The first integral in (15) expresses the energy of (4) in Ω, the second the energy in Ω_{T} (given $\gamma = 0$ in Ω_{T}). From the conditions for a stationary point of $\mathcal{L}$, we obtain the coupled problem in variational form

$$\begin{aligned} &\text{Seek } \; u \in \Lambda^{l-1}(\Omega), \;\; v \in \mathcal{T}(\Omega_{\mathrm{T}}): \\ &\int_\Omega \left(\star_\alpha \mathrm{d}u \wedge \mathrm{d}\eta + \star_\gamma u \wedge \eta \right) + (-1)^{l-1} \int_\Gamma \mathbf{t}\left(\star_\alpha \mathrm{d}v \right) \wedge \mathbf{t}\,\eta = (-1)^{l} \int_\Gamma \mathbf{t}\left(\star_\alpha \mathrm{d}w \right) \wedge \mathbf{t}\,\eta, \\ &(-1)^{l-1} \int_\Gamma \mathbf{t}\left(\star_\alpha \mathrm{d}\zeta \right) \wedge \mathbf{t}\, u + \int_{\Omega_{\mathrm{T}}} \star_\alpha \mathrm{d}\zeta \wedge \mathrm{d}v = \int_{\Omega_{\mathrm{T}}} \star_\alpha \mathrm{d}\zeta \wedge \mathrm{d}w \\ &\qquad \forall \eta \in \Lambda^{l-1}(\Omega),\, \forall \zeta \in \mathcal{T}(\Omega_{\mathrm{T}}). \end{aligned} \tag{16}$$

The same expression as (9) is obtained by noticing that

$$\int_{\Omega_{\mathrm{T}}} \star_\alpha \mathrm{d}\zeta \wedge \mathrm{d}v = -\left(-1\right)^{l-1} \int_\Gamma \mathbf{t}\left(\star_\alpha \mathrm{d}\zeta \right) \wedge \mathbf{t}\, v\,, \tag{17a}$$

$$\int_{\Omega_{\mathrm{T}}} \star_\alpha \mathrm{d}\zeta \wedge \mathrm{d}w = -\left(-1\right)^{l-1} \int_\Gamma \mathbf{t}\left(\star_\alpha \mathrm{d}\zeta \right) \wedge \mathbf{t}\, w\,, \tag{17b}$$

which hold by integration by parts because of $v, w \in \mathcal{T}(\Omega_\mathrm{T})$. Note that (17a) shows that $\mathbf{M}_\mathrm{T}$, which is its discrete representation, is a Hermitian positive-definite matrix and therefore invertible, which ensures that the Schur complement system (13) exists.

2.2. Coupling with a Trefftz Method through an $(m-1)$-Form

Now we exploit that $\mathrm{d}\mathbf{j} = 0$ in Ω_T, in order to switch to a potential representation; Ω_T is supposed to have trivial topology, i.e. m-th Betti number $\beta_m(\Omega_\mathrm{T}) = 0$ [27, p. 246, Theorem 2.1], given $m := n - l$. From (16) we derive a hybrid system for $u \in \Lambda^{l-1}(\Omega)$ and $\mathbf{j} \in \Lambda^m(\Omega_\mathrm{T})$ (with an abuse of notation) and introduce a potential form $\pi \in \Lambda^{m-1}(\Omega_\mathrm{T})$, which replaces the unknown $v \in \mathcal{T}(\Omega_\mathrm{T}) \in \Lambda^{l-1}(\Omega_\mathrm{T})$ in the exterior problem[3].

Based on (1a) and (1b), we can write that $\star_\alpha \mathrm{d}v = (-1)^l \mathbf{j}$ in Ω_T. (16) can therefore be rewritten as

$$\boxed{\begin{aligned}&\text{Seek } \; u \in \Lambda^{l-1}(\Omega), \;\; \mathbf{j} \in \mathcal{T}(\Omega_\mathrm{T}) \colon \\ &\int_\Omega (\star_\alpha \mathrm{d}u \wedge \mathrm{d}\eta + \star_\gamma u \wedge \eta) - \int_\Gamma \mathbf{t}\,\mathbf{j} \wedge \mathbf{t}\,\eta \;\; = (-1)^l \int_\Gamma \mathbf{t}\,(\star_\alpha \mathrm{d}w) \wedge \mathbf{t}\,\eta \\ &\qquad\qquad - \int_\Gamma \mathbf{t}\,\boldsymbol{\iota} \wedge \mathbf{t}\,u + \int_{\Omega_\mathrm{T}} \boldsymbol{\iota} \wedge \star_{\alpha^{-1}} \mathbf{j} = (-1)^l \int_{\Omega_\mathrm{T}} \boldsymbol{\iota} \wedge \mathrm{d}w \\ &\quad \forall \eta \in \Lambda^{l-1}(\Omega),\, \forall \boldsymbol{\iota} \in \mathcal{T}(\Omega_\mathrm{T}),\end{aligned}} \tag{18}$$

where $\mathbf{j}, \boldsymbol{\iota}$ belong to the same Trefftz space (7), after applying the transformation $v \to (-1)^l \star_\alpha \mathrm{d}v$ for functions $v \in \mathcal{T}(\Omega_\mathrm{T})$.

Let us now take $\pi, \tau \in \Lambda^{m-1}(\Omega_\mathrm{T})$ such that, in Ω_T, $\mathbf{j} = \star_\alpha \mathrm{d}\pi$ and $\boldsymbol{\iota} = \star_\alpha \mathrm{d}\tau$. This means that the new Trefftz space of functions that solve the exterior problem exactly is

$$\begin{aligned}\mathcal{T}(\Omega_\mathrm{T}) := \Big\{ v \in \Lambda^{m-1}(\Omega_\mathrm{T}) \colon \;\; &\mathrm{d}\,(\star_\alpha \mathrm{d}v) = 0\,, \;\; \alpha \in \mathbb{C}, \\ &v \text{ satisfies the condition at infinity (2)} \Big\},\end{aligned} \tag{19}$$

[3] In the case of $n = 3$, the unknown $v \in \Lambda^1(\Omega_\mathrm{T})$ is replaced by $\pi \in \Lambda^0(\Omega_\mathrm{T})$, i.e. a vector function is replaced by (the gradient of) a scalar function (see Section 3.2).

where $(m-1)$-forms are used instead of $(l-1)$-forms as in (7).

System (18) then becomes

$$\boxed{\begin{array}{l}\text{Seek } u \in \Lambda^{l-1}(\Omega),\ \ \pi \in \mathcal{T}(\Omega_{\mathrm{T}}):\\ \int\limits_{\Omega} (\star_\alpha \mathrm{d}u \wedge \mathrm{d}\eta + \star_\gamma u \wedge \eta) - \int\limits_{\Gamma} \mathbf{t}\,(\star_\alpha \mathrm{d}\pi) \wedge \mathbf{t}\,\eta = (-1)^l \int\limits_{\Gamma} \mathbf{t}\,(\star_\alpha \mathrm{d}w) \wedge \mathbf{t}\,\eta\\ \qquad - \int\limits_{\Gamma} \mathbf{t}\,(\star_\alpha \mathrm{d}\tau) \wedge \mathbf{t}\,u + \int\limits_{\Omega_{\mathrm{T}}} \star_\alpha \mathrm{d}\tau \wedge \mathrm{d}\pi \ = (-1)^l \int\limits_{\Omega_{\mathrm{T}}} \star_\alpha \mathrm{d}\tau \wedge \mathrm{d}w\\ \quad \forall \eta \in \Lambda^{l-1}(\Omega),\ \forall \tau \in \mathcal{T}(\Omega_{\mathrm{T}}),\end{array}} \tag{20}$$

where we can replace the integrals in Ω_{T} with integrals on Γ, similarly to (17).

3. Cell Method for Eddy-Current Problems

We specialize the problem of Section 2 for a frequency-domain eddy-current problem in $\mathbb{R}^3$, which amounts to the case $l = 2$ and $m = 1$. The electromagnetic fields involved – expressed with the customary notations – are the magnetic vector potential $\mathbf{A} : \mathbb{R}^3 \to \mathbb{C}^3$, the magnetic flux density $\mathbf{B} : \mathbb{R}^3 \to \mathbb{C}^3$, the magnetic field $\mathbf{H} : \mathbb{R}^3 \to \mathbb{C}^3$, and the current density $\mathbf{j} : \mathbb{R}^3 \to \mathbb{C}^3$. They correspond to the differential forms $u \in \Lambda^1(\mathbb{R}^3)$, $\boldsymbol{\sigma} \in \Lambda^2(\mathbb{R}^3)$, $\mathbf{j} \in \Lambda^1(\mathbb{R}^3)$, $\psi \in \Lambda^2(\mathbb{R}^3)$ of Section 2.

We also make use of material parameters $\nu, \sigma : \mathbb{R}^3 \to \mathbb{R}$ (reluctivity and conductivity) and $\omega \in \mathbb{R}$ (angular frequency). Written in Euclidean vector proxies of the forms [27, Section 2.2], the equilibrium equations become

$$\begin{cases} \nabla \times \mathbf{A} = \mathbf{B}, \\ \nabla \times \mathbf{H} = \mathbf{j}, \end{cases} \tag{21a}$$

and the constitutive equations

$$\begin{cases} \mathbf{H} = \nu \mathbf{B}, \\ \mathbf{j} = -\imath\omega\sigma \mathbf{A}, \end{cases} \tag{21b}$$

where $\imath$ is the imaginary unit. While ω is constant, the material parameters $\nu, \sigma : \mathbb{R}^3 \to \mathbb{R}$ generally vary in space. Note that ν and $-\imath\omega\sigma$ correspond to the Hodge operators $\star_\alpha$ and $\star_\gamma$ of Section 2.

The problem is completed[4] by the radiation condition [24, p. 259, Theorem 8.9]

$$\|\mathbf{A}\| = \mathcal{O}(\|\mathbf{x}\|^{-1}) \quad \text{for } \|\mathbf{x}\| \to \infty \text{ uniformly.} \tag{22}$$

We consider a domain $\Omega_\star$ such that, in the complement $\mathbb{R}^3 \setminus \Omega_\star$, we also have constant $\nu, \sigma \in \mathbb{R}$ ($\nu = \nu_\mathrm{T}$ and $\sigma = \sigma_\mathrm{T}$). Let us also introduce $\Omega \supset \Omega_\star$, $\Gamma := \partial\Omega$, in whose complement $\mathbb{R}^3 \setminus \Omega$ there is a known nonzero source $\mathbf{A}_0$, corresponding to the excitation $(l-1)$-form w of Section 2, which is given by the *Biot–Savart law* [13, p. 180, (5.28)]:

$$\mathbf{A}_0(\mathbf{x}) := \frac{\mu_0}{4\pi} \int\limits_{\Omega_0} \frac{\mathbf{j}_0(\mathbf{x}')}{\|\mathbf{x} - \mathbf{x}'\|} \, \mathrm{d}\mathbf{x}', \tag{23}$$

where $\mu_0 = 4\pi \cdot 10^{-7} \,\mathrm{H\,m^{-1}}$ and $\mathbf{j}_0 : \mathbb{R}^3 \to \mathbb{R}^3$ is the source current with support in some bounded Ω_0 and $\nabla \cdot \mathbf{j}_0 = 0$.

Furthermore, we assume that $\sigma = 0$ in $\mathbb{R}^3 \setminus \Omega$, which implies $\mathbf{j}|_{\mathbb{R}^3 \setminus \Omega} = 0$ and $\nabla \times \mathbf{H}|_{\mathbb{R}^3 \setminus \Omega} = \mathbf{0}$ from (21a) and (21b).

Next, we eliminate all other variables except for $\mathbf{A}$ in Ω:

$$\nabla \times (\nu \, \nabla \times \mathbf{A}) + \imath\omega\sigma\mathbf{A} = \mathbf{0} \,. \tag{24}$$

Taking the weak form of (24), we end up with a special case of (6), which we discretize following the cell method[5] by choosing a primal mesh $\mathcal{M}$ (and corresponding barycentric dual mesh $\widetilde{\mathcal{M}}$) in Ω.

Borrowing the notation from [9, 11, 12], we write the weak form of (24) in discrete form:

$$\left(\mathbf{C}^\mathsf{T} \mathbf{M}_\nu \mathbf{C} + \imath\omega \mathbf{M}_\sigma\right) \vec{\mathbf{a}} + \widetilde{\mathbf{C}}_\Gamma \widetilde{\mathbf{h}}_\Gamma = 0 \quad \text{in } \Omega \,. \tag{25}$$

- $\mathbf{C} \in \{-1, 0, 1\}^{N_\mathrm{faces}, N_\mathrm{edges}}$ is the incidence matrix from edges to faces of the primal mesh $\mathcal{M}$ in Ω (*discrete curl*). It corresponds to the exterior-derivative matrix $\mathbf{D}^{l-1}$ in (10).

[4] Note that we do not impose any gauge condition on $\mathbf{A}$, which is then not uniquely defined. Section 4, which presents numerical results, appropriately handles this issue.

[5] Instead of the cell method, we use FEM for discretization in [21, 23] and other works yet to be submitted (see Section 5).

- $\mathbf{M}_\nu \in \mathbb{R}^{N_{\text{faces}},N_{\text{faces}}}$ and $\mathbf{M}_\sigma \in \mathbb{R}^{N_{\text{edges}},N_{\text{edges}}}$ have entries $(\mathbf{M}_\nu)_{i,j} = \int_\Omega \nu(\mathbf{x})\, \mathbf{b}^{\text{f}}_i(\mathbf{x}) \cdot \mathbf{b}^{\text{f}}_j(\mathbf{x})\, \mathrm{d}\mathbf{x}$ and $(\mathbf{M}_\sigma)_{i,j} = \int_\Omega \sigma(\mathbf{x})\, \mathbf{b}^{\text{e}}_i(\mathbf{x}) \cdot \mathbf{b}^{\text{e}}_j(\mathbf{x})\, \mathrm{d}\mathbf{x}$, with $\mathbf{b}^{\text{f}}, \mathbf{b}^{\text{e}} \in \mathbf{L}^2(\Omega)$ piecewise-constant basis functions [14] that are linked to the intersections of, respectively, faces and edges between $\mathcal{M}$ and $\widetilde{\mathcal{M}}$. $\mathbf{M}_\nu$ and $\mathbf{M}_\sigma$ correspond to the mass matrices $\mathbf{M}^l_\alpha$ and $\mathbf{M}^{l-1}_\gamma$.

- $\vec{\mathbf{a}} \in \mathbb{C}^{N_{\text{edges}}}$ is the vector of line integrals of $\mathbf{A}$ on the edges of $\mathcal{M}$. It corresponds to vector $\vec{\mathbf{u}}$.

- $\widetilde{\mathbf{C}}_\Gamma \in \{-1,0,1\}^{\widetilde{N}_{\text{faces}},\widetilde{N}^{\text{bnd}}_{\text{edges}}}$ is the incidence matrix from boundary edges to faces of $\widetilde{\mathcal{M}}$ (faces of $\widetilde{\mathcal{M}}$ are related to edges of $\mathcal{M}$ because of duality). It corresponds to the matrix product $(-1)^{l-1} \left(\mathbf{T}^{l-1}_\Gamma\right)^{\mathsf{T}} \widetilde{\mathbf{K}}^{l-1}_{m,\Gamma}$.

- $\widetilde{\mathbf{h}}_\Gamma \in \mathbb{C}^{\widetilde{N}^{\text{bnd}}_{\text{edges}}}$ is the vector of line integrals of $\mathbf{H}$ on the boundary edges of $\widetilde{\mathcal{M}}$. It is a coupling term with the Trefftz domain.

3.1. Coupling with a Trefftz Method through the Magnetic Vector Potential

In the complement $\Omega_{\text{T}} := \mathbb{R}^3 \setminus \Omega$ we use Trefftz functions in

$$\boldsymbol{\mathcal{T}}(\Omega_{\text{T}}) := \Big\{ \mathbf{v} \in \mathbf{H}_{\text{loc}}(\mathbf{curl}, \Omega_{\text{T}}) \colon\ \nabla \times (\nabla \times \mathbf{v}) = \mathbf{0}\,,\ \nabla \cdot \mathbf{v} = 0\,, \\ \mathbf{v} \text{ satisfies the radiation condition (22)} \Big\}, \tag{26}$$

where $\mathbf{H}_{\text{loc}}(\mathbf{curl}, \Omega_{\text{T}}) := \{\mathbf{v} \in \mathbf{H}(\mathbf{curl}, \Omega_{\text{T}}) :\ f\mathbf{v} \in \mathbf{H}(\mathbf{curl}, \Omega_{\text{T}})\ \ \forall f \in C^\infty_{\text{c}}(\Omega_{\text{T}})\}$.

Transmission conditions become

$$\begin{cases} \mathbf{n} \times \left(\nu \nabla \times \mathbf{A}|_\Omega\right) = \mathbf{n} \times \left(\nu_{\text{T}} \nabla \times \mathbf{A}|_{\Omega_{\text{T}}}\right) & \text{(27a)} \\ \mathbf{n} \times \mathbf{A}|_\Omega = \mathbf{n} \times \mathbf{A}|_{\Omega_{\text{T}}} & \text{(27b)} \end{cases} \quad \text{on } \Gamma,$$

where $\mathbf{n}$ is the normal vector on Γ pointing from Ω_{T} to Ω.

$\mathbf{A}|_\Omega$ is discretized by the cell method and $\mathbf{A}|_{\Omega_{\text{T}}} = \mathbf{A}_{\text{T}} + \mathbf{A}_0$, where $\mathbf{A}_{\text{T}} \in \boldsymbol{\mathcal{T}}(\Omega_{\text{T}})$ and $\mathbf{A}_0$ is the known source (23).

We define a DtN matrix $\mathbf{P}_\Gamma \in \mathbb{C}^{\widetilde{N}^{\text{bnd}}_{\text{edges}},N_{\text{T}}}$ such that $\mathbf{P}_\Gamma \vec{\mathbf{v}} = \widetilde{\mathbf{h}}_\Gamma$, with $\vec{\mathbf{v}} \in \mathbb{C}^{N_{\text{T}}}$ vector of coefficients of Trefftz functions in the discrete space $\boldsymbol{\mathcal{T}}_n(\Omega_{\text{T}}) \in \boldsymbol{\mathcal{T}}(\Omega_{\text{T}})$ of dimension N_{T}, as follows:

$$(\mathbf{P}_\Gamma)_{i,j} := \nu_{\text{T}} \int_{\ell_i} \boldsymbol{\tau} \cdot (\nabla \times \mathbf{v}_j)\ \mathrm{d}\vec{\boldsymbol{s}}, \tag{28}$$

where ℓ_i, $i = 1, \dots, \widetilde{N}^{\text{bnd}}_{\text{edges}}$, is an edge of $\widetilde{\mathcal{M}}$ on Γ, $\boldsymbol{\tau}$ its tangential vector, and $\mathbf{v}_j$, $j = 1, \dots, N_{\text{T}}$, the Trefftz basis functions in $\boldsymbol{\mathcal{T}}_n(\Omega_{\text{T}})$.

We then plug (27a) into (25) by means of (28), impose (27b) weakly by multiplying it with $\mathbf{P}_\Gamma^\intercal \widetilde{\mathbf{C}}_\Gamma^\intercal$, and obtain the final discrete system

$$\boxed{\begin{aligned} \left(\mathbf{C}^\intercal \mathbf{M}_\nu \mathbf{C} + \imath\omega \mathbf{M}_\sigma\right) \vec{\mathbf{a}} + \widetilde{\mathbf{C}}_\Gamma \mathbf{P}_\Gamma \vec{\mathbf{v}} &= \widetilde{\mathbf{C}}_\Gamma \widetilde{\mathbf{h}}_{0,\Gamma} \\ \mathbf{P}_\Gamma^\intercal \widetilde{\mathbf{C}}_\Gamma^\intercal \vec{\mathbf{a}} - \quad \mathbf{M}_{\text{T}} \vec{\mathbf{v}} &= \mathbf{P}_\Gamma^\intercal \vec{\mathbf{b}}_{0,\Gamma} \end{aligned}} \tag{29}$$

which is a special case of (10). $\widetilde{\mathbf{h}}_{0,\Gamma} \in \mathbb{R}^{\widetilde{N}^{\text{bnd}}_{\text{edges}}}$ and $\vec{\mathbf{b}}_{0,\Gamma} \in \mathbb{R}^{N^{\text{bnd}}_{\text{faces}}}$ are, respectively, the vector of line integrals of $\mathbf{H}_0 := \nu_{\text{T}} \nabla \times \mathbf{A}_0$ on boundary edges of $\widetilde{\mathcal{M}}$ and the vector of fluxes of $\mathbf{B}_0 := \nabla \times \mathbf{A}_0$ on boundary faces of $\mathcal{M}$.

Thanks to the integral expression for the general case (9), $\mathbf{M}_{\text{T}}$ has entries

$$(\mathbf{M}_{\text{T}})_{i,j} := \nu_{\text{T}} \int_\Gamma \left[\mathbf{n} \times (\nabla \times \mathbf{v}_i)\right] \cdot \mathbf{v}_j \, \mathrm{d}S = -\nu_{\text{T}} \int_{\Omega_{\text{T}}} (\nabla \times \mathbf{v}_i) \cdot (\nabla \times \mathbf{v}_j) \, \mathrm{d}\mathbf{x}\,, \tag{30}$$

where the second equality holds because of the definition of $\boldsymbol{\mathcal{T}}(\Omega_{\text{T}})$ (26). Finally, the Schur complement of (29) is

$$\boxed{\left(\mathbf{C}^\intercal \mathbf{M}_\nu \mathbf{C} + \imath\omega \mathbf{M}_\sigma + \widetilde{\mathbf{C}}_\Gamma \mathbf{P}_\Gamma \mathbf{M}_{\text{T}}^{-1} \mathbf{P}_\Gamma^\intercal \widetilde{\mathbf{C}}_\Gamma^\intercal\right) \vec{\mathbf{a}} = \widetilde{\mathbf{C}}_\Gamma \widetilde{\mathbf{h}}_{0,\Gamma} + \widetilde{\mathbf{C}}_\Gamma \mathbf{P}_\Gamma \mathbf{M}_{\text{T}}^{-1} \vec{\mathbf{b}}_{0,\Gamma}\,.} \tag{31}$$

3.2. Coupling with a Trefftz Method through the Magnetic Scalar Potential

We can simplify the matrices in (31) by imposing $\beta_1(\Omega_{\text{T}}) = 0$ [27, p. 252, Lemma 2.2] (compare with Section 2.2), which is always allowed because Γ is defined by the user. Hence, we introduce a magnetic scalar potential ϕ in Ω_{T}, which corresponds to $\pi \in \Lambda^0(\Omega_{\text{T}})$ of Section 2.2. The constitutive equations for the exterior problem become

$$\begin{cases} \mathbf{H} = \nu_{\text{T}} \nabla \phi & \text{(32a)} \\ \nabla^2 \phi = 0 & \text{(32b)} \end{cases} \quad \text{in } \Omega_{\text{T}},$$

with the radiation condition

$$\phi = \mathcal{O}(\|\mathbf{x}\|^{-1}) \quad \text{for } \|\mathbf{x}\| \to \infty \text{ uniformly.} \tag{33}$$

Transmission conditions are

$$\begin{cases} \mathbf{n} \times \left(\nu \nabla \times \mathbf{A}|_{\Omega} \right) = \mathbf{n} \times \left(\nu_{\mathrm{T}} \nabla \phi|_{\Omega_{\mathrm{T}}} \right) & \text{(34a)} \\ \mathbf{n} \cdot \left(\nabla \times \mathbf{A}|_{\Omega} \right) = \mathbf{n} \cdot \left(\nabla \phi|_{\Omega_{\mathrm{T}}} \right) & \text{(34b)} \end{cases} \quad \text{on } \Gamma.$$

As before, there is a known source ϕ_0 in Ω_{T} such that $\phi|_{\Omega_{\mathrm{T}}} = \phi_{\mathrm{T}} + \phi_0$, $\phi_{\mathrm{T}} \in \mathcal{T}(\Omega_{\mathrm{T}})$. The Trefftz space is

$$\begin{aligned} \mathcal{T}(\Omega_{\mathrm{T}}) := \Big\{ & v \in H^1_{\mathrm{loc}}(\Omega_{\mathrm{T}}) \colon \ \nabla^2 v = 0 \,, \\ & v \text{ satisfies the radiation condition (33)} \Big\}. \end{aligned} \tag{35}$$

In particular, we choose the Trefftz basis functions

$$v_{\mathsf{lm}}(r_{xc}, \theta_{xc}, \varphi_{xc}) = r_{xc}^{-\mathsf{l}-1} Y_{\mathsf{lm}}(\theta_{xc}, \varphi_{xc}), \quad \mathsf{l} = 0, \ldots, \infty, \quad \mathsf{m} = -\mathsf{l}, \ldots, \mathsf{l}, \tag{36}$$

which fulfill the definition of multipoles given in Section 1.2. Here, $(r_{xc}, \theta_{xc}, \varphi_{xc})$ are spherical coordinates ($r \in [0, \infty)$, $\theta \in [0, 2\pi)$, $\varphi \in [0, \pi]$) of the vector $\mathbf{x}_c := \mathbf{x} - \mathbf{c}$, with $\mathbf{c}$ center of the multipole. $Y_{\mathsf{lm}}(\theta, \varphi)$ are spherical harmonics [13, p. 107, Section 3.5].

Thanks to (34a), we can rewrite the DtN matrix (28) as

$$\mathbf{P}_\Gamma := \widetilde{\mathbf{G}}_\Gamma \mathbf{R}_\Gamma \,, \quad (\mathbf{R}_\Gamma)_{i,j} := \nu_{\mathrm{T}} \, v_j(\widetilde{\mathbf{x}}_i). \tag{37}$$

$\widetilde{\mathbf{G}}_\Gamma \in \{-1, 0, 1\}^{N^{\mathrm{bnd}}_{\mathrm{edges}}, N^{\mathrm{bnd}}_{\mathrm{nodes}}}$ is the incidence matrix from nodes to edges of $\widetilde{\mathcal{M}}$ on Γ. v_j, $j = 1, \ldots, N_{\mathrm{T}}$, are the chosen multipoles (36), while $\widetilde{\mathbf{x}}_i$, $i = 1, \ldots, \widetilde{N}^{\mathrm{bnd}}_{\mathrm{nodes}}$, are the nodes of $\widetilde{\mathcal{M}}$ on Γ (which correspond to the centroids of the faces of $\mathcal{M}$ on Γ, using a barycentric dual mesh).

We can also rewrite the energy matrix $\mathbf{M}_{\mathrm{T}}$ in (29) as

$$(\mathbf{M}_{\mathrm{T}})_{i,j} := -\nu_{\mathrm{T}} \int_\Gamma (\mathbf{n} \cdot \nabla v_i) \; v_j \; \mathrm{d}S = -\nu_{\mathrm{T}} \int_{\Omega_{\mathrm{T}}} \nabla v_i \cdot \nabla v_j \; \mathrm{d}\mathbf{x} \,. \tag{38}$$

4. Numerical Results

We provide a numerical example for the eddy-current equation (24) with the radiation condition (22) and $\omega = 0$ in $\mathbb{R}^3$ (*magnetostatics*). This problem is

solved for the magnetic vector potential $\mathbf{A}$ in Ω using the cell method and the magnetic scalar potential ϕ in Ω_{T} using multipoles (36). The source is given by (23), where $\mathbf{j}_0$ is tangential to a circular loop in Ω_{T} (which is Ω_0 in (23)), with $\|\mathbf{j}_0\| = 1000\,\mathrm{A}$.

We take the same axisymmetric domain of [12, Section V.A]. Ω is then composed of

1. $\Omega_\star$, which is a cylinder with a cylindrical hole and $\nu = 1/(k\mu_0)$, with $k \in \mathbb{R}$ and $\mu_0 = 4\pi \cdot 10^{-7}\,\mathrm{H\,m^{-1}}$: we simulate for $k = 2$ and $k = 4000$, the latter being typical of practical applications (like iron). $\Omega_\star$ is also surrounded by
2. an *air box* with $\nu = 1/\mu_0$.

The boundary Γ does not therefore coincide with any material interface.

To show that the coupling is not much affected by the shape of Γ as long as it is artificial, we consider two geometries for the air box: a cylinder and a sphere. For geometric details refer to Figure 1. The corresponding 3D meshes are shown in Figure 2.

Consequently, for each air box we consider a different configuration of multipoles:

1. Multipoles up to order 1, i.e. (36) for $\mathsf{l} = 0, \mathsf{m} = 0$ and $\mathsf{l} = 1, \mathsf{m} = -1, 0, 1$, whose centers are uniformly arranged on a cylinder with radius $0.02\,\mathrm{m}$ and height $0.04\,\mathrm{m}$ (the bottom face lies on the XY-plane). The number of centers is set proportional to the (rounded) logarithm of the number of intersections of entities of the mesh on Γ.
2. Multipoles up to order 4, all in the center of the spherical air box. This configuration leads to a diagonal matrix $\mathbf{M}_{\mathrm{T}}$ because of the orthogonality of spherical harmonics [13, p. 108, (3.55)].

Our code is written in `MATLAB R2016b`, using an iterative solver applied to the Schur complement (31). Note that we use an iterative solver not only for its computational efficiency, but also because we have to: in case $\omega = 0$, the

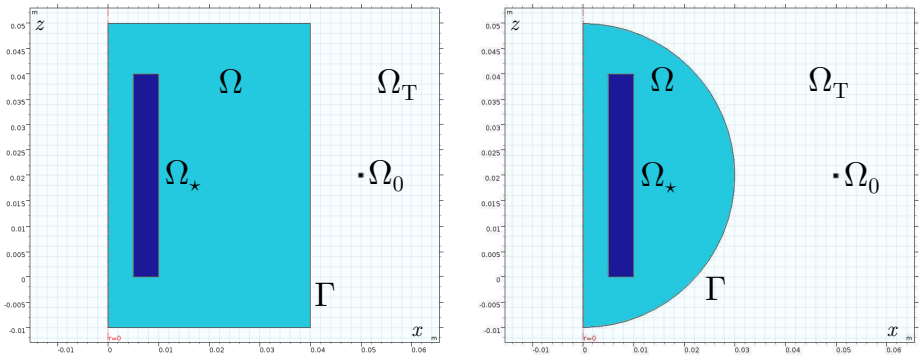

(a) Cylindrical air box with radius 0.04 m and height 0.06 m (the bottom face lies on the plane $z = -0.01$ m).

(b) Spherical air box with radius 0.03 m centered in $(0, 0, 0.02\,\text{m})$.

Figure 1: Geometries of Ω and Ω_0 for the axisymmetric example: slices parallel to the positive XZ-plane. The cylinder forming $\Omega_\star$ has radius 0.01 m and height 0.04 m (the bottom face lies on the plane $z = 0$), while its cylindrical hole has radius 0.005 m. The circumference on the XY-plane forming Ω_0 (shown as a point in the figures) has radius 0.05 m and lies on the plane $z = 0.02$.

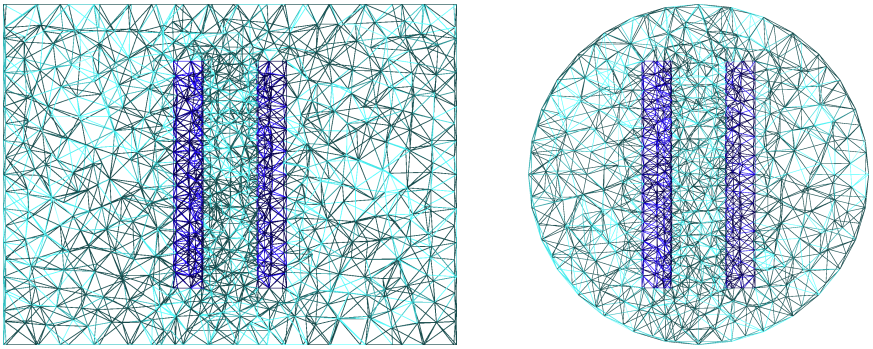

(a) Number of tetrahedrons = 29 447.

(b) Number of tetrahedrons = 19 648.

Figure 2: Meshes of Ω for the axisymmetric example: slices parallel to the XZ-plane.

solution is not unique without a gauge for the magnetic vector potential in Ω, which we do not impose under the cell method. However, the right-hand side of the problem is divergence-free on the discrete level (for the cell method, the discrete divergence is an incidence matrix), as it stems from the (continuous) source (23) with null divergence: hence, the solution returned by iterative solvers lies in a Krylov subspace that is also divergence-free and the Coulomb gauge

$$\nabla \cdot \mathbf{A} = 0 \quad \text{in } \Omega \tag{39}$$

is implicitly imposed.

The iterative solver used is the *minimum residual method* (`minres`) with a *symmetric successive over-relaxation* preconditioner [28, p. 37, Section 3.3] given by $(\mathbf{D}_{11} + \mathbf{L}_{11})\,\mathbf{D}_{11}^{-1}\,(\mathbf{D}_{11} + \mathbf{L}_{11})^{\mathsf{T}}$, with $\mathbf{D}_{11}, \mathbf{L}_{11} \in \mathbb{R}^{N_{\text{edges}}, N_{\text{edges}}}$ diagonal and lower-triangular parts, respectively, of the top-right block (pure cell method) of (29), i.e. $\mathbf{C}^{\mathsf{T}}\mathbf{M}_{\nu}\mathbf{C}$. Figure 3 shows convergence for both configurations of multipoles: the spherical air box makes the solver achieve the desired tolerance of 10^{-11} slightly faster, which is due to the fact that $\mathbf{M}_{\mathrm{T}}$ is diagonal. While the convergence is reached more slowly for $k = 4000$ (Figure 3b), the total number of iterations is still not too different from $k = 2$ (Figure 3a). This holds even though, with a more pronounced physical discontinuity, the ill-conditioning of the system gets worse because of the large difference in scale between the matrix entries inside and outside $\Omega_{\star}$.

The *transpose-free quasi-minimal residual method* (`tfqmr`) also converges with the same preconditioner, but after a few more iterations.

We test the implementation with a benchmark solution returned by `COMSOL Multiphysics 5.3`, which also provides the meshes. This solution is produced by 3$^{\text{rd}}$-order vector FEM on a very refined mesh of a spherical air box of radius 0.6 m (20 times larger than the radius of the spherical air box of Figure 1b) centered in $(0, 0, 0.02\,\text{m})$. Dirichlet boundary conditions ($\mathbf{n}\times\mathbf{A} = \mathbf{0}$) are imposed on the air box boundary. The time spent by `COMSOL` to produce this solution on an ordinary computer is comparable to the time spent by our `MATLAB` code: up to 10 seconds in both cases.

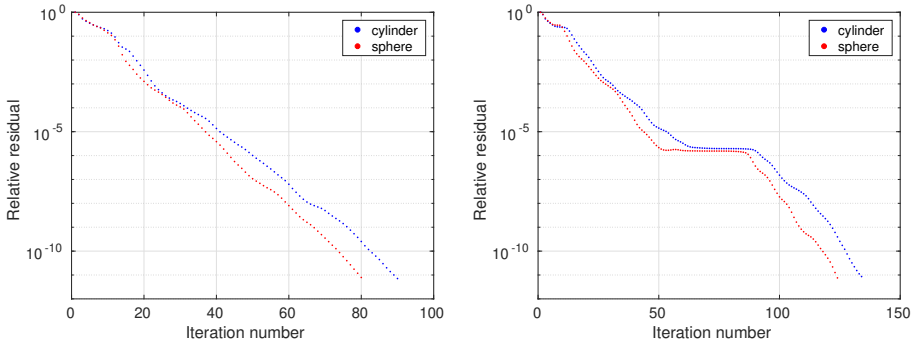

(a) $\nu_\star = 1/(2\mu_0)$ (b) $\nu_\star = 1/(4000\mu_0)$

Figure 3: Plots of relative residual norms vs. iteration numbers for `minres`. Relative residual norms are defined as $\|\mathbf{b} - \mathbf{A}\mathbf{x}_i\|/\|\mathbf{b}\|$ for the linear problem $\mathbf{A}\mathbf{x} = \mathbf{b}$, with i iteration number. The y-axis (relative residual norms) is in logarithmic scale.

Figures 4 and 5 for $k = 2$ and Figures 6 and 7 for $k = 4000$ compare the x and z Cartesian components of the magnetic flux density resulting from the coupling with the benchmark solution. The magnetic flux density is computed by interpolating magnetic fluxes, easily obtainable from the degrees of freedom of the cell method ($\vec{\mathbf{a}}$ in (25)), by means of Whitney basis functions: it is then plotted over the segment with corners $(0.0025\,\mathrm{m}, 0, 0)$ and $(0.0025\,\mathrm{m}, 0, 0.04\,\mathrm{m})$, which is inside the hole of $\Omega_\star$. Comparing with the benchmark solution, the accuracy for the spherical air box is better than the cylindrical (especially for $\mathbf{B}_z$), even though the cylindrical air box is larger than the spherical (and less elements have been used for discretization: see Figure 2). This holds for both values of k considered.

On the other hand, to investigate convergence we choose an example with a smooth exact solution and set $k = 1$, such that the hollow cylinder $\Omega_\star$ is also filled with air. Here, the uniformly-meshed domain Ω does not contain an internal boundary, as the one between solid-colored regions in Figure 1. For both the cylindrical and spherical air boxes, the number of multipoles is set proportional to the logarithm of the meshwidth h on Γ.

The exact solution is given by the Biot–Savart law (23). With respect to

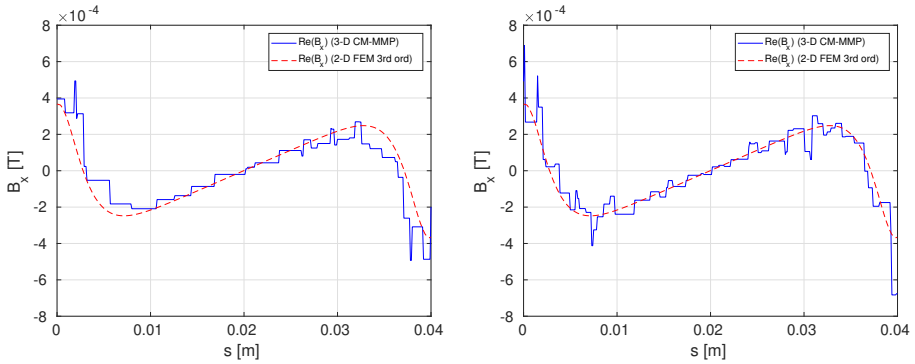

(a) Cylindrical air box with multipoles on internal cylinder.

(b) Spherical air box with multipoles in the center.

Figure 4: Value of $\mathbf{B}_x$ along $[(0.0025\,\mathrm{m}, 0, 0), (0.0025\,\mathrm{m}, 0, 0.04\,\mathrm{m})]$ (s parametrizes the z-coordinate), given $\nu_\star = 1/(2\mu_0)$.

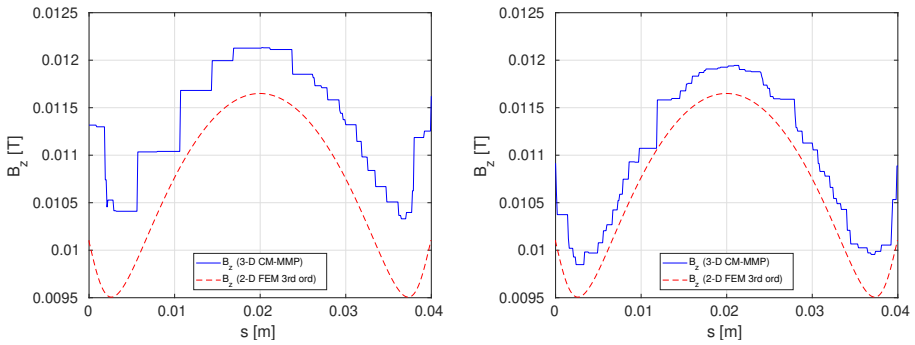

(a) Cylindrical air box with multipoles on internal cylinder.

(b) Spherical air box with multipoles in the center.

Figure 5: Value of $\mathbf{B}_z$ along $[(0.0025\,\mathrm{m}, 0, 0), (0.0025\,\mathrm{m}, 0, 0.04\,\mathrm{m})]$ (s parametrizes the z-coordinate), given $\nu_\star = 1/(2\mu_0)$.

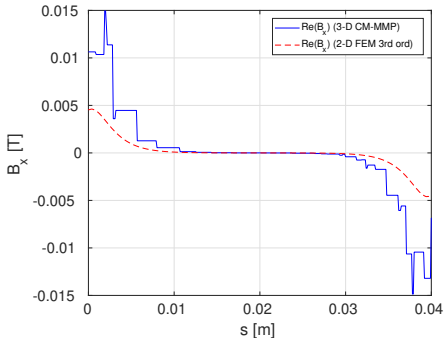

(a) Cylindrical air box with multipoles on internal cylinder.

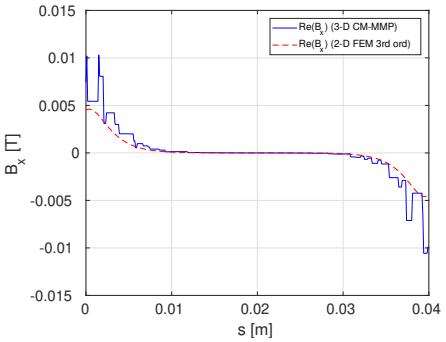

(b) Spherical air box with multipoles in the center.

Figure 6: Value of $\mathbf{B}_x$ along $[(0.0025\,\mathrm{m}, 0, 0)\,, (0.0025\,\mathrm{m}, 0, 0.04\,\mathrm{m})]$ (s parametrizes the z-coordinate), given $\nu_\star = 1/(4000\mu_0)$.

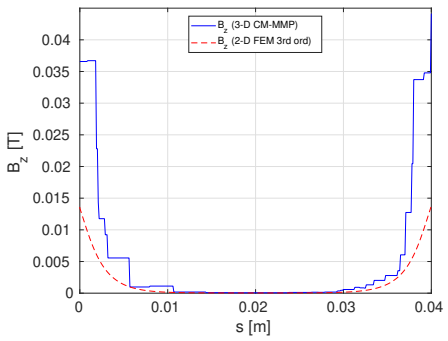

(a) Cylindrical air box with multipoles on internal cylinder.

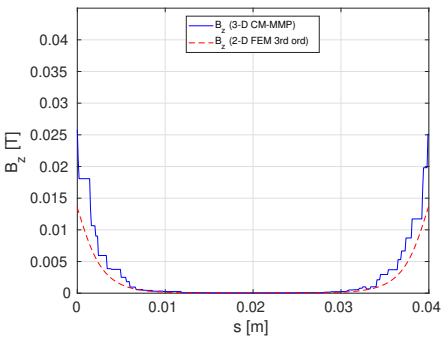

(b) Spherical air box with multipoles in the center.

Figure 7: Value of $\mathbf{B}_z$ along $[(0.0025\,\mathrm{m}, 0, 0)\,, (0.0025\,\mathrm{m}, 0, 0.04\,\mathrm{m})]$ (s parametrizes the z-coordinate), given $\nu_\star = 1/(4000\mu_0)$.

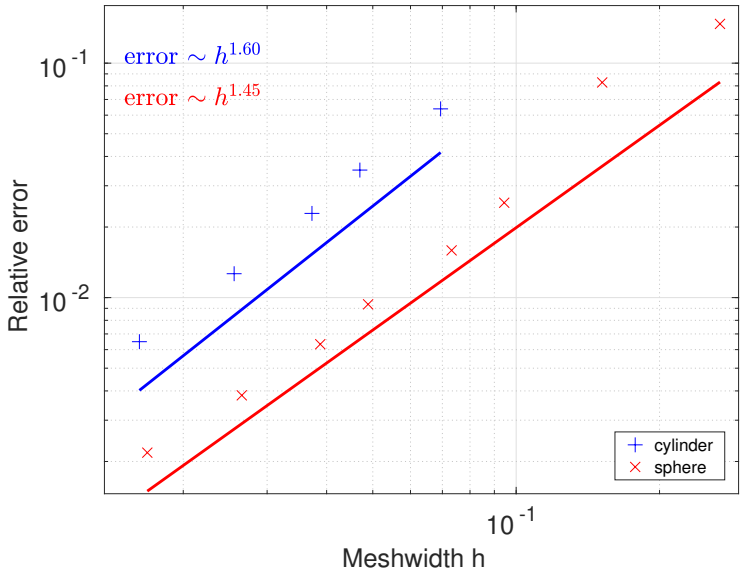

Figure 8: h-refinement log-log plots of relative errors of $\mathbf{A}$ in $\mathbf{H}(\mathbf{curl}, \Omega)$-seminorm.

it, we compute errors in a discrete $\mathbf{H}(\mathbf{curl}, \Omega)$-seminorm arising from the cell method, whose degrees of freedom are line integrals of $\mathbf{A}$ on the meshes ($\vec{\mathbf{a}}$): specifically, we compute ℓ^2-errors between $\vec{\mathbf{b}} := \mathbf{C}\vec{\mathbf{a}}$ and the face fluxes of $\mathbf{B}_0 := \nabla \times \mathbf{A}_0$ from the Biot–Savart law (23).

Figure 8 shows the results of this h-refinement convergence test, presenting algebraic convergence with approximately the same rate for both the cylindrical and spherical air boxes. Note that there are more datapoints for the latter because an acceptable numerical solution is produced even with very coarse meshes of a sphere.

5. Conclusion

The authors are not aware of any prior work addressing the coupling of Trefftz methods with a framework for numerical schemes based on volume meshes, like co-chain calculus. We explain for the first time how to formulate a boundary term for this framework that takes into account the exterior problem. The particular case of coupling the cell method with MMP is also presented here for

the first time.

Compared to other hybrid approaches that rely on BEM, coupling with a Trefftz method enjoys several advantages [29, p. 51], namely a simpler assembly process, as there are no singular integrals, and exponential convergence when the coupling boundary is far from field singularities. This entails a small number of degrees of freedom for the Trefftz method that permits to compute the Schur complement of the final system.

Acknowledgements

This work was supported by the Swiss National Science Foundation [grant number 2000021_165674/1].

We acknowledge Jasmin Smajic, Institute for Energy Technology, Hochschule für Technik Rapperswil, for putting the authors in contact through a research exchange to the University of Padova.

References

[1] R. Hiptmair, Discrete Hodge operators, Numerische Mathematik 90 (2) (2001) 265–289. doi:10.1007/s002110100295.

[2] R. Hiptmair, Discrete Hodge-operators: an algebraic perspective, Progress In Electromagnetics Research 32 (2001) 247–269. doi:10.2528/PIER00080110.

[3] A. Bossavit, 'Generalized finite differences' in computational electromagnetics, Progress In Electromagnetics Research 32 (2001) 45–64. doi:10.2528/PIER00080102.

[4] D. N. Arnold, R. S. Falk, R. Winther, Finite element exterior calculus, homological techniques, and applications, Acta Numerica 15 (2006) 1–155. doi:10.1017/S0962492906210018.

[5] A. N. Hirani, Discrete exterior calculus, PhD thesis, California Institute of Technology (May 2003).

[6] E. Schulz, G. Tsogtgerel, Convergence of discrete exterior calculus approximations for Poisson problems, Discrete & Computational Geometry.

[7] E. Tonti, A direct discrete formulation of field laws: the cell method, CMES - Computer Modeling in Engineering and Sciences 2 (2) (2001) 237–258.

[8] E. Tonti, Finite formulation of electromagnetic field, IEEE Transactions on Magnetics 38 (2) (2002) 333–336. doi:10.1109/20.996090.

[9] L. Codecasa, Refoundation of the cell method using augmented dual grids, IEEE Transactions on Magnetics 50 (2) (2014) 497–500. doi:10.1109/TMAG.2013.2280504.

[10] P. Alotto, M. Guarnieri, F. Moro, A boundary integral formulation on unstructured dual grids for eddy-current analysis in thin shields, IEEE Transactions on Magnetics 43 (4) (2007) 1173–1176. doi:10.1109/TMAG.2006.890948.

[11] F. Moro, L. Codecasa, Indirect coupling of the cell method and BEM for solving 3-D unbounded magnetostatic problems, IEEE Transactions on Magnetics 52 (3) (2016) 1–4. doi:10.1109/TMAG.2015.2487822.

[12] F. Moro, L. Codecasa, A 3-D hybrid cell boundary element method for time-harmonic eddy current problems on multiply connected domains, IEEE Transactions on Magnetics 55 (3) (2019) 1–11.

[13] J. D. Jackson, Classical Electrodynamics, 3rd Edition, Wiley, New York, NY, 1999.

[14] L. Codecasa, F. Trevisan, Piecewise uniform bases and energetic approach for discrete constitutive matrices in electromagnetic problems, International Journal for Numerical Methods in Engineering 65 (4) (2005) 548–565. doi:10.1002/nme.1457.

[15] F. Moro, D. Desideri, A. Doria, A. Maschio, C. Medé, L. Codecasa, A face-smoothed cell method for static and dynamic piezoelectric coupled prob-

lems on polyhedral meshes, Journal of Computational Physics 386 (2019) 84–109. doi:10.1016/j.jcp.2019.02.012.

[16] M. Bebendorf, Approximation of boundary element matrices, Numerische Mathematik 86 (4) (2000) 565–589. doi:10.1007/PL00005410.
URL https://doi.org/10.1007/PL00005410

[17] R. Hiptmair, A. Moiola, I. Perugia, A Survey of Trefftz Methods for the Helmholtz Equation, Springer, Cham, 2016, pp. 237–279. doi:10.1007/978-3-319-41640-3_8.
URL https://doi.org/10.1007/978-3-319-41640-3_8

[18] C. Hafner, Chapter 3 - The Multiple Multipole Program (MMP) and the Generalized Multipole Technique (GMT), in: T. Wriedt (Ed.), Generalized Multipole Techniques for Electromagnetic and Light Scattering, Mechanics and Mathematical Methods–Series of Handbooks, Elsevier, Amsterdam, 1999, pp. 21–38. doi:10.1016/B978-044450282-7/50015-4.

[19] B. Carrascal, G. A. Estevez, P. Lee, V. Lorenzo, Vector spherical harmonics and their application to classical electrodynamics, European Journal of Physics 12 (4) (1991) 184–191. doi:10.1088/0143-0807/12/4/007.

[20] P. R. S. Antunes, A numerical algorithm to reduce ill-conditioning in meshless methods for the Helmholtz equation, Numerical Algorithms 79 (3) (2018) 879–897. doi:10.1007/s11075-017-0465-z.

[21] Coupling finite elements and auxiliary sources, Computers & Mathematics with Applications 77 (6) (2019) 1513–1526. doi:10.1016/j.camwa.2018.09.007.

[22] J. Smajic, C. Hafner, J. Leuthold, Coupled FEM-MMP for computational electromagnetics, IEEE Transactions on Magnetics 52 (3) (2016) 1–4. doi:10.1109/TMAG.2015.2475241.

[23] D. Casati, R. Hiptmair, J. Smajic, Coupling finite elements and auxiliary sources for Maxwell's equations, International Journal of Numerical Modelling: Electronic Networks, Devices and Fieldsdoi:10.1002/jnm.2534.

[24] W. McLean, Strongly Elliptic Systems and Boundary Integral Equations, 1st Edition, Cambridge University Press, Cambridge, 2000.

[25] P. Monk, Finite Element Methods for Maxwell's Equations, 1st Edition, Numerical Mathematics and Scientific Computation, Clarendon Press, Oxford, 2003. doi:10.1093/acprof:oso/9780198508885.001.0001.

[26] K. Sakakibara, Analysis of the dipole simulation method for two-dimensional Dirichlet problems in Jordan regions with analytic boundaries, BIT Numerical Mathematics 56 (4) (2016) 1369–1400. doi:10.1007/s10543-016-0605-1.

[27] R. Hiptmair, Finite elements in computational electromagnetism, Acta Numerica 11 (2002) 237–339. doi:10.1017/S0962492902000041.

[28] R. Barrett, M. Berry, T. F. Chan, J. Demmel, J. Donato, J. Dongarra, V. Eijkhout, R. Pozo, C. Romine, H. Van der Vorst, Templates for the Solution of Linear Systems: Building Blocks for Iterative Methods, 2nd Edition, SIAM, Philadelphia, PA, 1994.

[29] D. I. Kaklamani, H. T. Anastassiu, Aspects of the Method of Auxiliary Sources (MAS) in computational electromagnetics, IEEE Antennas and Propagation Magazine 44 (3) (2002) 48–64. doi:10.1109/MAP.2002.1028734.